

# Simulation of atmospheric cascade including vacuum excitation and Higgs production

Kalyanee Boruah

*Department of Physics, Gauhati University, Guwahati-781014, India*

(Received 6 August 1996)

We consider here a new mechanism for multiparticle production in the simulation of a cosmic ray cascade in the atmosphere. The mechanism is the decay of Higgs particles that are produced through vacuum excitation in a cosmic ray collision. We develop a model of hadronic interaction based on the GENCL code of the UA5 experiment, incorporating a fraction of energy transfer to bubble formation by phase transition due to vacuum excitation and subsequent multiparticle production via conversion of Higgs particles to heavy fermion pairs. Such events are expected to have high multiplicity and excess muons. We compare the muon multiplicity distribution with and without this effect for different fractions of energy transfer going to Higgs boson production. Our results show that signatures of Higgs boson production may be seen above the primary energy  $10^{17}$  eV, with an increasing fraction of energy transfer as we go to higher energies. [S0556-2821(97)04923-0]

PACS number(s): 13.85.Tp, 14.80.Bn, 96.40.De

## I. INTRODUCTION

The search for Higgs particles has been one of the prime interests of present and future accelerators. This particle is predicted by the Salam-Weinberg spontaneous symmetry-breaking theory and its production mechanism is explained by local vacuum destabilization and bubble formation by phase transition [1]. As a result of high-energy collision- in cosmic ray events, there is the possibility that the vacuum becomes locally hot; Higgs particles are produced and decay very fast to heavy fermion pairs. This effect is manifested in a very rapid increase of the multiplicity of charged hadrons with energy. The possibility of vacuum excitation depends on the fraction of the total energy of the collision that goes to local excitation and bubble formation. This fraction and its dependence on energy is not known. In the present paper, we develop a model assuming different fractions of center-of-mass energies producing vacuum excitation and Higgs particles, combined with a nonsingle diffractive event generator based on the GENCL code of the UA5 experiment [2]. The temperature dependence of the vacuum and the mechanism of bubble formation is described by Mishra *et al.* [1], using the thermofield theory of Umezawa, Matsumoto, and Tachiki [3]. They obtained temperature-dependent effective potentials and Higgs boson masses using a variational and nonperturbative methodology. In our model of multiparticle production, we have used their results and considered several decay modes and branching ratios for the Higgs boson decay based on recent particle review data [4]. This part is described in Sec. II. In Sec. III, we describe the basic features of the interaction model used to develop the Monte Carlo code to simulate the hadronic cascade. This is based on previous work [5], incorporating multiple hadron production by means of a multicluster model reproducing the observed features at collider energies and extended to include the nuclear target effects. In the present analysis, the interaction and decay processes in the atmosphere are simulated only for hadrons ( $\pi$ ,  $K$ , and  $N$ ) and muons above 5 GeV. Subroutines are developed for the production and decay processes of the hadrons and Higgs particles and are coupled to the cascade program in order to generate muon events, to which most of the

hadrons and Higgs particles finally decay. In Sec. IV, we discuss the results of the simulation of the muon multiplicity distribution for different fractions of energy transfer and their significance at different primary energies.

## II. HIGGS BOSON PRODUCTION THROUGH VACUUM EXCITATION

### A. Vacuum destabilization and bubble formation

The temperature dependence of the vacuum and the mechanism of bubble formation is theoretically studied by Mishra *et al.* considering the nonperturbative mechanism for the production of Higgs particles through vacuum excitation. Vacuum destabilization can occur if enough energy is pumped into a small macroscopic volume which thermalizes locally and forms a bubble having a nonzero temperature and local thermal equilibrium. The total energy of such a locally excited region or bubble shall be given as

$$E_b = \int \Delta \epsilon[\beta(r)] dr, \quad (1)$$

where  $\Delta \epsilon(\beta)$  is the gap in energy density and  $\beta = 1/kT$  is spatially dependent. The number of Higgs particles inside the bubble is given by

$$n_H = \int N[\beta(r)] dr, \quad (2)$$

where  $N(\beta)$  is the number density of the Higgs particles at temperature  $\beta$  (see the Appendix). The temperature distribution inside the bubble is taken as

$$\beta(r)^{-1} = T(r) = T_0 \exp(-ar^2), \quad (3)$$

where  $T_0$  is the temperature at the center of the bubble and the parameter  $a$  decides the region over which the vacuum is excited, with the volume being approximately  $a^{-3/2}$  (volume of the bubble). Here, the volume is estimated from the length scale associated with the cross section of the collision process:

$$\sigma \approx \pi/a. \quad (4)$$

In the energy range  $E=10^{15}-10^{18}$  eV, the cross section is estimated from extrapolation resulting from the dual parton model (DPM) [6]:

$$\sigma_{pp}^{\text{inel}} = 0.314 \log^{1.8} s + 23, \quad (5)$$

where  $s$  is the square of the center-of-mass energy in  $\text{GeV}^2$ . The number of wounded target nucleons hit by the projectile depends on the target mass number  $A$  and is given by [6]

$$\langle n_T \rangle = [0.56 + 0.0236 \log(s - 1.76)] A_{\text{target}}^{0.31}. \quad (6)$$

As the bubble cools, the Higgs particles will get more massive and decay to heavy fermion pairs. The mass of the Higgs particle at the instant of decay is determined at random from a uniform distribution between 0 and  $T_0$ .

Numerical calculations (see the Appendix) give the multiplicity of Higgs particles  $n_H$  and bubble energy  $E_b$  as a function of central temperature  $T_0$ . The values of  $n_H$  are correlated with  $E_b$  and the results are parametrized approximately as

$$\langle n_H \rangle = 2.312 + 2.418 E_b, \quad (7)$$

where  $E_b$  is in TeV.

### B. The model

Assuming a given primary energy of proton ( $E_p = 10^{15}-10^{18}$  eV) and a given fraction ( $fh=0-0.5$ ) of the energy transfer for vacuum excitation and bubble formation, first bubble energy  $E_b$  ( $=\sqrt{s} \cdot fh$ ) is calculated for each event. Then the mean number of Higgs bosons corresponding to bubble energy  $E_b$  is calculated from the parametrization (7), and the actual number ( $N_b$ ) for a particular event is chosen from a Poisson distribution with this mean. The bubble energy is divided between these  $N_b$  bosons and the mass ( $E_b/N_b$ ) corresponds to the final mass as the bubble cools to zero temperature. The central temperature  $T_0$  is determined from the calculation of  $E_b$  vs  $T_0$  as described above. The temperature at which a particular Higgs boson will decay is determined at random from a uniform distribution between 0 and  $T_0$ . The corresponding Higgs boson mass at this temperature is determined from the calculation of the Higgs boson mass versus bubble temperature  $T$  (see the Appendix).

The choice of a particular decay channel is made depending on the simulated Higgs boson mass ( $m_H$ ), using the most prominent recent data [3]:

- (i)  $m_H < m_W$ ,  $H \rightarrow b\bar{b}$  ( $\sim 90\%$ ),  $\tau^+ \tau^-$  ( $\sim 10\%$ ).
- (ii)  $m_W < m_H < m_Z$ ,  $H \rightarrow b\bar{b}$  ( $\sim 80\%$ ),  $WW$  ( $\sim 10\%$ ),  $\tau^+ \tau^-$  ( $\sim 10\%$ ).
- (iii)  $m_Z < m_H < 2m_W$ ,  $H \rightarrow b\bar{b}$  ( $\sim 80\% - 10\%$ ),  $WW^*$  ( $10\% - 97\%$ ),  $ZZ^*$  ( $\sim 0\% - 10\%$ ).
- (iv)  $2m_W < m_H < 2m_Z$ ,  $H \rightarrow WW$  ( $\sim 100\%$ ).
- (v)  $m_H > 2m_Z$ ,  $H \rightarrow WW$  ( $\sim 70\%$ ),  $ZZ$  ( $\sim 30\%$ ).

The  $WW$  and  $ZZ$  channels further decay to electrons, muons, and neutrinos according to  $W \rightarrow e\nu$ ,  $\mu\nu$  or  $Z \rightarrow e^+e^-$ ,  $\mu^+\mu^-$ .  $b\bar{b}$  channels also either directly decay to muons or electrons (10%) or indirectly via intermediate states  $\tau^+ \tau^-$ ,

$\pi^+ \pi^-$ ,  $2\pi^0$ , etc. The respective branching ratios are calculated from the recent particle data review [4].  $\tau^+ \tau^-$  decay modes are decided by individual channels:

$$\tau^- \rightarrow \mu^- \nu_{\bar{\nu}} (\sim 18\%), e^- \nu_{\bar{\nu}} (\sim 17\%), h^- \nu_{\bar{\nu}} (\sim 52\%). \quad (8)$$

The muon number is calculated from the direct and indirect channels via the decay of the hadrons. In the present model, the muon multiplicity is calculated by considering only the various decay channels leading to muons.

### III. INTERACTION MODEL

According to recent theoretical [7] and experimental [2] considerations, in the hadron-air interaction model, the particles are produced in clusters. The Monte Carlo simulation program is written following the algorithm of the GENCI code developed at CERN, by the UA5 Collaboration, including the effect of nuclear target mass. High-energy nucleon-nucleon interactions may be classified as diffractive [single diffractive (SD) and double diffractive (DD) and nondiffractive (ND)]. In ND events, particles are produced in a central region, flat in rapidity and in two fragmentation regions, where the leading particles emerge. In the diffractive events, at least one of the nucleons is excited to higher mass diffractive systems and decay independently. The fraction of SD events is about 10% at intersecting storage ring (ISR) energies [8], decreasing to about 8.5% at CERN collider energies (UA4 Collaboration). In the present study for cosmic ray interactions, we consider only nondiffractive events. Here an event is built up of two leading and a varying number of central clusters. Each cluster is given a transverse momentum  $p_T$  and a rapidity  $y$ . After transforming the rapidities to conserve energy and momentum, the clusters are made to decay isotropically. The Monte Carlo algorithm is based on the following processes.

(i) The number of charged hadrons are chosen from a negative binomial distribution, with the following parameters:

$$\langle n_{\text{ch}} \rangle = -7.0 + 7.2s^{0.127}, \quad (9)$$

$$k^{-1} = -0.104 + 0.058 \ln(\sqrt{s}). \quad (10)$$

(ii) The basic multiparticle production mechanism is by cluster formation and decay. Out of the six different types of clusters, we consider only three, viz., pion, kaon, and the leading cluster, excluding the less frequent nucleon, hyperon, and  $X_i$  pairs. The nature of the leading particles ( $p$  or  $n$ ) is chosen considering the charge exchange probability as given in [2].

(iii) Kaons are grouped into pairs (clusters) of zero strangeness including pairs with neutral Kaons and with Kaon resonances [2]. The pairs  $K^+ K^-$ ,  $K^+ \bar{K}^0$ ,  $K^0 K^-$ , and  $K^0 \bar{K}^0$  have all the same production probability and each Kaon is a  $K^*$  with 60% probability, according to CERN Intersecting Storage Rings (ISR) measurements [9]. The actual number of Kaon clusters is drawn from a Poisson with a mean deduced from the  $K/\pi$  ratio:

$$R_k = \langle K^\pm \rangle / \langle \pi^\pm \rangle = 0.024 + 0.0062 \ln(s). \quad (11)$$

The  $K^{*}$ 's decay into  $K\pi$  pairs:  $K^{*0} \rightarrow K^0\pi^0(\frac{1}{3}), K^+\pi^-(\frac{2}{3});$   $K^{*+} \rightarrow K^0\pi^+(\frac{1}{3}), K^+\pi^0(\frac{2}{3})$ .  $K^0$ 's are considered as  $K_S^0$  and  $K_L^0$  with equal probability. All  $K^0$ 's,  $K^\pm$ , and pions finally decay to muons and electrons and their decay are governed by standard branching ratios.

(iv) The remaining charged particles are  $\pi^+$  and  $\pi^-$ . They are put together with  $\pi^0$ 's into clusters. The algorithm [2] is based on drawing the number of charged pions from a Poisson distribution with an average of 1.8, repeatedly until there are no charged particles left and then drawing  $\pi^0$ 's from an independent Poisson distribution with the following parameter:

$$\mu_{\pi^0} = [0.5(2 + 1.03n_{\text{ch}}) - 0.4\mu_k]/n_c, \quad (12)$$

where  $\mu_k = [R_k/(1 + R_k)]n'_{\text{ch}}$ ,  $n'_{\text{ch}}$  is the number of charged particles left to be simulated, and  $n_c$  is the number of pion clusters.

(v) All clusters made up of more than one particle are given some excitation energy in terms of an additional mass. For kaon clusters, this is chosen from an exponential distribution:

$$\frac{dN}{dE^2} \propto \exp(-2E/b), \quad (13)$$

where the parameter  $b$  has the value 0.75 GeV for kaon clusters. The pion clusters are given masses  $m$  from the following distribution:

$$\frac{dN}{dm} = 1.1[1 + N_0(0,0.2)]\exp[(1/3)n_\pi - 1], \quad (14)$$

where  $n_\pi$  is the total number of pions in the cluster and  $N_0(0,0.2)$  is a number drawn from a Gaussian distribution with mean 0 and standard deviation 0.2 GeV.

(vi) The clusters are then given transverse momentum  $p_T$  and longitudinal momentum  $p_L$  in two steps following the GENCL code: The transverse momenta are randomized from either an exponential distribution

$$\frac{dN}{dp_T^2} \propto \exp(-b \cdot p_T), \quad (15)$$

where  $b = 6 \text{ GeV}/c$  or from an inverse power-law distribution

$$\frac{dN}{dp_T^2} \propto \frac{1}{(P_T + P_0)^\alpha}, \quad (16)$$

$$p_0 = 3 \text{ GeV}/c, \quad \alpha = 3 + 1/[0.01 + 0.011 \ln(s)]. \quad (17)$$

For the single pion clusters,  $p_T$  is always sampled from the exponential distribution. In the other cases, the relative amount of the two distributions is made to depend on the multiplicity of the event. For  $p$ -air interactions, these distributions are multiplied by the parameter:

$$R(p_T) = 0.0363p_T + 0.057 \quad \text{for } p_T \leq 4.52 \text{ GeV}/c. \quad (18)$$

The azimuthal angles of the leading nucleons and of the meson clusters are chosen randomly between 0 and  $2\pi$ . To conserve momenta in the  $x$ - $y$  plane perpendicular to the beam axis ( $z$  direction) two independent linear translations are made in the components of  $p_T$ :

$$p_i^{\text{new}} = p_i^{\text{old}} - \left( \sum p_i^{\text{old}} \right) / N, \quad i = x, y, \quad (19)$$

where the summation is over  $N$  clusters in the event. Longitudinal momentum is given to a cluster by assigning to it a rapidity  $y$ :

$$p_L = m_T \sinh(y) \quad (20)$$

where  $m_T = \sqrt{(m^2 + p_T^2)}$  is the transverse mass. Rapidity distributions have a central plateau and a fall off at higher values of  $|y|$ , and can be described analytically by two Gaussian peaks [10], with the following parameters [11]:

$$s_1 = 0.146 \ln(E_p) + 0.164,$$

$$\sigma_1 = 0.120 \ln(E_p) + 0.255.$$

Rapidities are generated by the Box-Muller method and the two leading clusters are given the highest and lowest rapidities. They are converted to longitudinal momenta  $p_L$  and so adjusted as to conserve total momentum and energy, after assigning a fraction  $\langle k \rangle$  (inelasticity parameter  $\sim 0.5$ ) of available energy to the leading nucleons.

(vii) Each cluster with given energy is made to decay via the available channels with probability proportional to their respective branching ratios. The number of muons above threshold energy 5 GeV are counted for each event.

#### IV. RESULT AND DISCUSSION

The simulation program is run for primary energies  $E_p(10^{15} - 10^{18} \text{ eV})$  with different fractions  $fh$  ( $= 0 - 0.5$ ) of energy transfer to bubble formation. The resulting multiplicity distributions for 1000 simulations each are compared with corresponding simulations with  $fh = 0$ . Results are summarized in Figs. 1–3. It is seen that the Higgs boson mechanism has a significant effect starting from  $E_p = 10^{17} \text{ eV}$ , as shown by the respective  $\chi^2$  values (Fig. 3). It may be noted that the present mechanism of Higgs particle production consists of three parts: (i) formation of the bubble, (ii) production of Higgs particles by temperature-dependent vacuum depending on quantum-mechanical behavior, and (iii) dissipation of the bubble through particle production via conversion of Higgs particles to heavy fermion pairs. In the present analysis we have concentrated on the last part, by applying the parametrization to the phenomenological model of ultra high energy (UHE) cosmic ray interaction in the atmosphere. In order to derive signatures of Higgs boson production, high-energy muons above 5 GeV are selected as the probe, as they are less interacting particles giving direct information about the first nuclear interactions, and may be observed at ground level. However, the energy dependence of the fraction of energy transfer needs to be investigated in more detail, as well as the time scales involved with bubble formation for a detailed four-dimensional simulation.

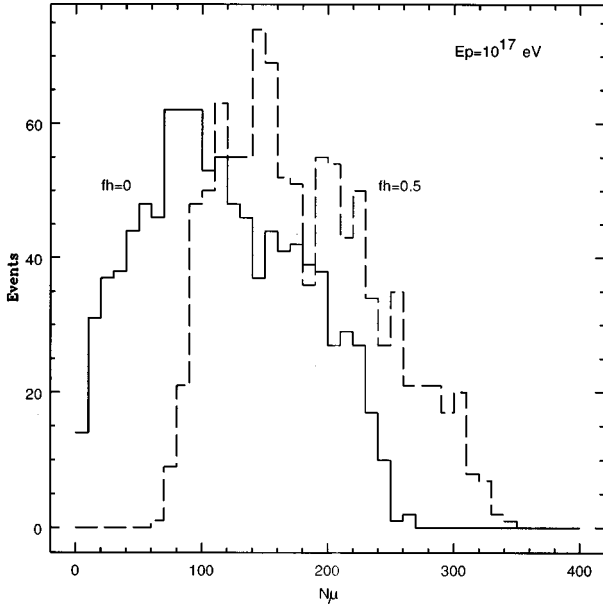


FIG. 1. Muon multiplicity distributions for 1000 showers with  $E = 10^{17}$  eV.

#### ACKNOWLEDGMENTS

The author is grateful to Professor S. P. Misra, for introducing theoretical concepts and to Professor J. V. Narlikar for allowing me to use the excellent computing and library facility of the Inter University Centre for Astronomy and Astrophysics at Pune. Financial support from the Board of Research in Nuclear Sciences, Department of Atomic Energy, Government of India is also acknowledged.

#### APPENDIX: TEMPERATURE DEPENDENCE OF VACUUM

In the nonperturbative solution of field theory, the ground state  $|\text{vac}'\rangle$  is defined as the state of lowest energy corre-

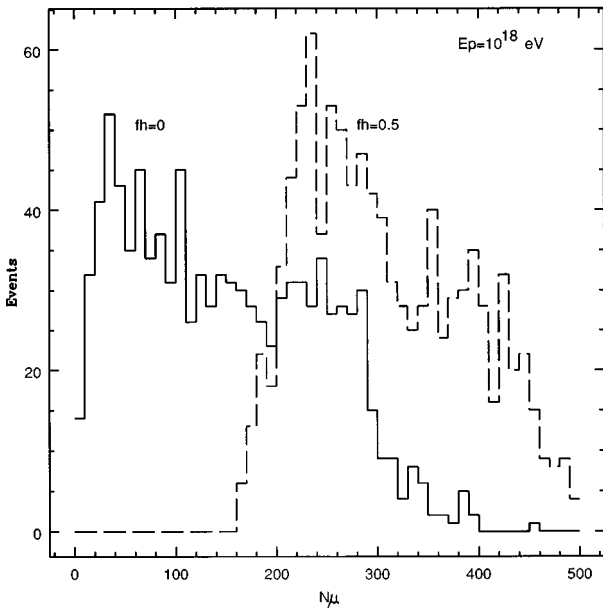


FIG. 2. Muon multiplicity distributions for 1000 showers with  $E = 10^{18}$  eV.

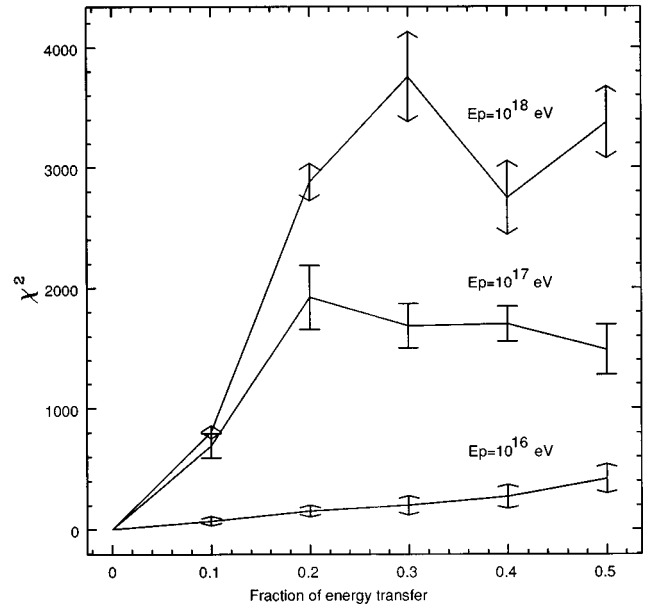


FIG. 3. Deviations of simulation from the distribution with  $fh = 0$ .

sponding to zero temperature and the expectation value of the Hamiltonian density is given by

$$\epsilon_0 = \langle \text{vac}' | \tau^{00} | \text{vac}' \rangle = -\frac{1}{2} m^2 \xi^2 + (\lambda/4) \xi^4. \quad (\text{A1})$$

A minimization of the energy density  $\epsilon_0$  with respect to  $\xi$  gives the result  $\xi = \xi_0 = [m^2/\lambda]^{1/2}$ . Now, this can be generalized to finite temperature by using the methodology of thermofield dynamics [3]. The thermal vacuum is given by

$$|\text{vac}', \beta\rangle = U(\beta) |\text{vac}'\rangle \quad (\text{A2})$$

where  $\beta = 1/kT$ . If  $\tau_{\text{eff}}^{00}$  is the effective Hamiltonian density, then the energy density at temperature  $\beta$  will become

$$V(\xi, \beta) = \epsilon(\beta) = \langle \text{vac}', \beta | \tau_{\text{eff}}^{00} | \text{vac}', \beta \rangle \quad (\text{A3})$$

$$\begin{aligned} &= \frac{1}{2} (2\pi)^{-3} \int \frac{\omega(k, \beta)^2 + k^2 + 3\lambda \xi^2 - m^2}{\omega(k, \beta) \{ \exp[\beta \omega(k, \beta)] - 1 \}} dk \\ &+ \frac{3\lambda}{4} \left[ (2\pi)^{-3} \int \frac{dk}{\omega(k, \beta) \{ \exp[\beta \omega(k, \beta)] - 1 \}} \right]^2 \\ &+ \frac{\lambda}{4} \xi^4 - \frac{m^2}{2} \xi^2, \end{aligned} \quad (\text{A4})$$

where  $\omega(k, \beta) = [k^2 + m_H(\beta)^2]^{1/2}$ , with  $m_H(\beta)$  being the Higgs boson mass at temperature  $1/\beta$ . In the thermofield method, temperature-dependent field theory needs the physical mass of the Higgs particle as input while using the distribution function in the calculation of temperature-dependent effective potential as in the right-hand side of Eq. (A4) through  $\omega(k, \beta)$ . Now if we follow the method of defining the mass through the second derivative of the effective potential at its minimum, then for a given input mass  $[m_H(\beta)]$  on the right-hand side of Eq. (A4), first  $V(\xi, \beta)$  is evaluated and  $\xi_{\text{min}}$  corresponding to the minimum of effective potential is estimated. With this value, the square root of the expression  $|d^2 V(\xi, \beta)/d\xi^2|_{\xi=\xi_{\text{min}}}$  gives the output mass. Self-consistency demands that both be the same.

We determine  $m_H(\beta)$  in Eq. (A4) through an iterative procedure until the input mass equals the output mass.

For numerical evaluation, it is useful to rewrite Eq. (A4) in terms of the dimensionless quantities with the substitutions  $z = \xi/\xi_0$ ,  $\mu = m_H(\beta)/\xi_0$ ,  $y = \beta\xi_0$ , and  $x = k/\xi_0$ , where  $\xi_0$  is the value of  $\xi_{\min}$  at zero temperature. The expression for the effective potential now becomes

$$V(z, y) = \xi_0^4 \left[ \frac{\lambda}{4} z^4 - \frac{\lambda}{2} z^2 + \frac{1}{2} I_1(z, y) + \frac{3\lambda}{4} [I_2(z, y)]^2 \right] = \xi_0^4 V_1(z, y), \quad (\text{A5})$$

$$I_1(z, y) = \frac{1}{2\pi^2} \int_0^\infty \frac{x^2 [\omega(x)^2 + x^2 + \lambda(3z^2 - 1)]}{\omega(x) \{ \exp[y\omega(x)] - 1 \}} dx, \quad (\text{A6})$$

$$I_2(z, y) = \frac{1}{2\pi^2} \int_0^\infty \frac{x^2 dx}{\omega(x) \{ \exp[y\omega(x)] - 1 \}}, \quad (\text{A7})$$

where  $\omega(x) = (x^2 + \mu^2)^{1/2}$ . The effective potential is calculated as a function of  $\xi$  and  $\beta$  and a plot of  $V(\xi) = V(\xi, \beta)$

$-V(0, \beta)$  as a function of  $\xi$  shows a double well structure and a change of shape for  $T = T_c \approx 2.1\xi_0$ , which determines the critical temperature.

Calculations give the values of Higgs boson mass [ $m_H(\beta)$ ] in  $\xi_0$  unit as a function of  $T$ . Starting with a maximum at  $T=0$ ,  $m_H$  falls to 0 at  $T=T_c$ . However, it again rises for  $T>T_c$ . A plot of  $\xi_{\min}$  and  $d^2V/d\xi^2|_{\xi=0}$  shows that critical temperature is  $T_c = 2.1\xi_0 \approx 525$  GeV, in agreement with the results of Dolan and Jackiew [12]. The field expectation value corresponding to the minimum of the potential comes out to have a value of  $\xi_0 \approx 250$  GeV.

The gap in the energy density of the thermal vacuum with respect to the vacuum at zero temperature is given by

$$\Delta \epsilon(\beta) = V(\xi_{\min}, \beta) - V(\xi_{\min}, \beta = \infty) = \xi_0^4 [V_1(z_{\min}, y) + \lambda/4]. \quad (\text{A8})$$

The number density of Higgs particles at temperature  $\beta$  is given as

$$N(\beta) = (2\pi)^{-3} \int \frac{dk}{\exp[\beta\omega(k, \beta)] - 1}. \quad (\text{A9})$$

- 
- [1] A. Mishra, H. Mishra, S. P. Misra, and S. N. Nayak, Phys. Rev. D **44**, 110 (1991).  
 [2] UA5 Collaboration, G. J. Alner *et al.*, Nucl. Phys. **B291**, 445 (1987).  
 [3] H. Umezawa, H. Matsumoto, and M. Tachiki, *Thermofield Dynamics and Condensed States* (North-Holland, Amsterdam, 1982).  
 [4] Particle Data Group, R. M. Barnett *et al.*, Phys. Rev. D **54**, 1 (1996).  
 [5] C. Forti *et al.*, Phys. Rev. D **42**, 3668 (1990).  
 [6] J. N. Capdevielle *et al.*, Kernforschungszentrum, Karlsruhe Report No. 4998, 1992 (unpublished), p. 10.

- [7] A. Giovannini and L. Van Hove, Acta Phys. Pol. B **19**, 495 (1988).  
 [8] G. Giacomelli and M. Jacob, Phys. Rep. **55**, 1 (1979).  
 [9] AFS Collaboration, T. Akesson *et al.*, Nucl. Phys. **B203**, 27 (1982).  
 [10] A. Klar and J. Hufner, Phys. Rev. D **31**, 491 (1985).  
 [11] J. N. Capdevielle, in *Cosmic Rays 94: Solar Heliospheric, Astrophysical and High-Energy Aspects*, Proceedings of the European Symposium, Balatonfured, Hungary, edited by G. Erdos *et al.* [Nucl. Phys. B (Proc. Suppl.) **39A**, 154 (1995)].  
 [12] I. Dolan and R. Jackiew, Phys. Rev. D **9**, 3320 (1974).